Catalytic reaction rates in thermodynamically non-ideal systems

Rostam J. Madon [a], Enrique Iglesia [b]

[a] *Engelhard Corporation, Iselin, NJ 08830, USA*
[b] *Department of Chemical Engineering, University of California at Berkeley, Berkeley, CA 94720, USA*

This manuscript is dedicated to Professor Michel Boudart, our teacher as graduate students and our trusted advisor since.

Abstract

Chemical reactions reflect the universal tendency of systems to approach equilibrium. The dynamics towards equilibrium, reflected in rates of chemical reactions, are therefore influenced only by thermodynamic properties, such as reaction affinity and the chemical potential, activity, or fugacity of reactants and products. Reaction rates depend on concentrations only in ideal reaction mixtures, because here, concentration appears in the defining equations for all relevant thermodynamic properties. Catalytic reactions in gas–liquid–solid systems involve molecules solvated in a non-ideal environment and reacting on surfaces. Transition state treatments show that such reactions on surfaces detect the presence and identity of a liquid phase only when a liquid solvates kinetically relevant adsorbed intermediates and activated complexes or when its presence prevents gas–liquid equilibrium by imposing transport restrictions.

Chemisorption energies are much larger than typical intermolecular interactions in liquids; therefore, inert liquids rarely influence the structure or reactivity of chemisorbed reactants and activated complexes. However, solvent effects become possible on heterogeneous catalysts when adsorption or desorption steps are rate-determining or kinetically relevant. Here, the reaction coordinate involves molecules in solution, and the corresponding activated complexes can become solvated by the surrounding fluid phase. In the special case of identical solvation of a reactant and an activated complex, a fortuitous cancellation of activity coefficients leads to reaction rates that depend on concentration rather than the thermodynamic activity of reactants. This stringent requirement makes concentration-driven reaction rates unusual exceptions to the general case of chemical reaction rates that depend on the thermodynamic activity of reactants and products.

We have used transition state treatments of reaction rates in non-ideal systems to explain observed solvent effects for cyclohexene hydrogenation on Pt and Pd catalysts. A dihydrogen dissociative-adsorption rate-determining step on Pt leads to solvation of the kinetically relevant activated complex. Its activity coefficient and that for dissolved H_2 cancel. As a result, the hydrogenation rate on Pt depends on H_2 concentration in the liquid phase. On Pd, the rate-determining step involves chemisorbed species that are not influenced by the solvent; the reaction rate depends only on H_2 partial pressure in the gas phase and not on the nature of the liquid. A similar treatment shows that the presence of liquid products in three-phase Fischer–Tropsch synthesis reactors cannot increase the rate of olefin readsorption, unless the liquid introduces transport restrictions that prevent rapid removal of olefins from catalyst pores. Higher solubility of larger olefins cannot account for enhanced readsorption. In fact, increasing solubility either has no effect or, under certain circumstances, increases the propensity for desorption rather than readsorption. Finally, we show mechanistic implications of the dependence of paraffin

E-mail addresses: rostam.madon@engelhard.com (R.J. Madon), iglesia@cchem.berkeley.edu (E. Iglesia).

cracking rates on intrazeolite paraffin activities or concentrations. For example, for dependence on the latter, we involve a molecule in a precursor state that is solvated by the environment within zeolite channels to the same extent as a paraffin absorbed within the structure. Since zeolites introduce non-ideality to a reaction system, experimental observations need to be rationalized using the approach we have proposed. © 2000 Elsevier Science B.V. All rights reserved.

Keywords: Catalytic reactions; Non-ideal systems; Transition state theory; Cyclohexene hydrogenation; Zeolite catalysis; Fischer–tropsch synthesis

---

1. Introduction

Chemical reaction rates are often described as functions of concentrations of reactants and products in reacting mixtures. Reaction and diffusion rates, however, reflect the tendency of chemical and physical systems to approach thermodynamic equilibrium. Therefore, the kinetic driving force that rigorously determines these rates depends on thermodynamic properties, such as reaction affinity (A), and chemical potential (μ) or activity (a) of kinetically relevant species [1–5]. Concentrations (C) appear in the defining equations for thermodynamic properties only in the limiting case of thermodynamic ideality. As a result, chemical reaction rates contain concentration terms only for ideal systems, where fugacities (f) and concentrations may be accurately interchanged in rate expressions.

1.1. Catalytic reactions in non-ideal systems

Condensed phases within multiphase gas–liquid–solid catalytic reactors and gaseous components near their condensation point place reactants and products within thermodynamically non-ideal environments. Here, non-ideality does not reflect the documented effects of reactive solvents on adsorbed species, but the ubiquitous case of a liquid or gas phase that engenders intermolecular interactions in the fluid phase, without influencing the chemical properties of a catalytic surface or adsorbed intermediates. A simple illustration of such phenomena is the use of inert solvents to disperse catalyst particles and to dissolve reactants in three-phase reactors. In such systems, concentrations of reactants, which differ markedly between a contacting gas phase and an inert liquid phase, are not relevant kinetic variables.

Consider a three-phase reactor in which a solid dispersed in an inert liquid catalyzes the conversion of gaseous reactants dissolved in the same inert liquid. In the absence of gas–liquid transport restrictions, equilibrium exists between gas and liquid phases, and the chemical potential for each reactant and product species becomes identical in the two fluid phases. Therefore, a reaction must occur at identical rates whether reactants reside in the gas phase or within an inert liquid, as long as the liquid does not influence the nature of the kinetically relevant adsorbed species or activated complexes. These conclusions become less obvious if a liquid influences the catalytic properties of a surface, for example by solvating the activated complex involved in one or more of the kinetically relevant elementary steps.

Solvation of catalytic entities occurs quite frequently in reactions catalyzed by homogeneous solvated metal complexes [6,7]. Here, the solvent is seldom inert, as it solvates a catalyst molecule via chemical interactions with ligands around active metal centers. Reactions catalyzed by solvated homogeneous complexes often involve rate-determining steps requiring ligand displacements and the attachment (oxidative addition) and detachment (reductive elimination) of reacting molecules, which themselves are solvated by the liquid. As a result, solvent molecules are intimately involved in catalytic turnovers and invariably influence the stability of activated complexes of most elementary steps. Consequently, solvent effects are quite prevalent in chemical reactions catalyzed by solvated organometallic complexes [6,7]. In such cases, activity coefficients (γ) for reactants and for activated complexes often cancel, and reaction rates become functions of the concentration of reactants and products even under non-ideal conditions.

In heterogeneous catalysis, the role of solvents and conditions that effectuate intermolecular interactions and result in thermodynamically non-ideal reaction environments remains unclear and controver-

sial. Binding energies of adsorbed species involved in catalytic reactions significantly exceed typical energies of intermolecular interactions in a fluid phase. Therefore, in most cases, a fluid phase will not influence significantly the structure and reactive events of surface species. Exceptions to this conclusion arise if rate-determining steps involve adsorption (entry) or desorption (exit) steps, because their corresponding activated complexes may be solvated by the surrounding fluid phase. In this paper, we apply the tenets of transition state theory for non-ideal systems in order to illustrate, via three examples, the practical consequences of using thermodynamic properties to describe the kinetics of chemical reactions on heterogeneous catalysts.

1.2. Transition state theory in thermodynamically non-ideal systems

For an elementary reaction, $A + B \rightarrow$ products, transition state theory postulates that the reaction rate r per unit volume is proportional to the number of activated complexes per unit volume ($C_{\ddagger}$) crossing the activation barrier with a frequency ν_b [4,8].

$$r = \nu_b C_{\ddagger} \tag{1}$$

The complex is considered to be a molecule with the assumed composition and structure, but with its normal vibrational motion along the bond being broken or formed (the reaction coordinate) excluded from its thermodynamic description. The symbol $\ddagger$ denotes the activated complex or transition state. Equation (1) contains the concentration of the activated complex not its thermodynamic activity or fugacity. For chemical reactions in thermodynamically non-ideal systems, as shown elsewhere [4,8,9], the rate becomes

$$r = \frac{k_B T}{h} K^{\ddagger} \frac{a_A a_B}{\gamma_{\ddagger}} = k_0 \frac{\gamma_A \gamma_B}{\gamma_{\ddagger}} C_A C_B \tag{2}$$

$$K^{\ddagger} = \frac{a_{\ddagger}}{a_A a_B} \tag{3}$$

where $K^{\ddagger}$ is the equilibrium constant for the conversion of reactants in the ground state to an activated complex, in which all degrees of freedom except vibration along the reaction coordinate are included in its thermodynamic description. In these expressions, k_B

is the Boltzmann's constant; h, the Planck's constant; and T, the temperature. Also, k_0 is the rate constant for thermodynamically ideal systems and is described by the Brønsted–Bjerrum relation:

$$k = k_0 \frac{\gamma_A \gamma_B}{\gamma_{\ddagger}} \tag{4}$$

Boudart [4] has reviewed the consequences of thermodynamic non-ideality for dilute strong electrolytes. Using the Debye–Huckel theory for reactions between two ions A and B in dilute strong electrolytes, Eqs. (2) and (3) lead to the experimentally observed dependence of rate constants on the ionic strength of the liquid phase. In contrast, an expression for r that is merely proportional to the activity product for the two reactants, and which does not account for the activity coefficient of the activated complex and its solvation by the liquid phase, is unable to describe the experimental results. Clearly, the number of activated complexes undergoing a reactive vibration per unit volume, and not the thermodynamic activity of the activated complexes doing so, determines the reaction rate. This fact has often, and incorrectly, been taken out of context in order to justify the use of concentrations of reactants and products in reaction rate expressions. Eq. (2) clearly shows that reaction rates depend on the thermodynamic activities of reactants in a given elementary step.

For reactions at high pressures in a non-ideal gas phase, Eckert and Boudart [10] also showed that Eq. (2) is the correct expression for the rate of a homogeneous gas phase reaction in a non-ideal environment. For such systems, Eq. (4) may be re-written as

$$k = k_0 \frac{\phi_A \phi_B Z}{\phi_{\ddagger}} \tag{5}$$

where ϕ is the fugacity coefficient and Z is the compressibility factor for the gas mixture. For the homogeneous decomposition of hydrogen iodide, $2HI \rightarrow H_2 + I_2$ at high pressures, Eckert and Boudart [10] showed that the observed complex dependence of the rate on HI partial pressure reflects the non-ideal nature of the gas phase. They obtained a pressure-independent rate coefficient over a wide range of HI pressures by using Eqs. (2) and (5). If the fugacity of the activated complex was used instead of its concentration in Eq. (1), as suggested by Whalley [11], rate coefficients varied significantly with HI pressure and hence with the severity of non-ideality of the reactant mixture.

These studies [4,10] have shown that Eq. (2) accurately describes reaction rates in thermodynamically non-ideal systems. All analyses of reaction rates for chemical reactions must therefore start with Eqs. (1) and (2) and with concepts embodied within the transition state theory.

2. Rate-determining and kinetically relevant elementary steps

The definition of chemical equilibrium requires that a solute in equilibrium with its vapor must have the same chemical potential in the liquid and gas phases [5]. Therefore, for a solvent to influence the rate of a chemical reaction, it must also influence the activated complex of the rate-determining step (rds), or in the absence of one, the activated complexes for any steps whose rate constants appear in the overall rate expression for a chemical reaction. In the classical definition of Horiuti [12], the rate-determining step is the only exergic step with a positive reaction affinity ($A_i > 0$) in a cycle, and all other steps are quasi-equilibrated ($A_i = 0$). When a rate-determining step exists, its rate constants, forward and reverse, are the only ones appearing in the rate expression; all other rate constants appear as equilibrium ratios or not at all. For quasi-equilibrated adsorption–desorption steps, when liquid and gas phases are in equilibrium, one obtains surface concentrations that are identical and independent of the surrounding phase.

Many catalytic cycles, however, are described by more than one exergic step. Boudart and Tamaru [13] have proposed that the rate of an irreversible catalytic cycle containing more than one exergic step is controlled by the one step whose rate constant is the only one appearing in the overall rate expression. In such cases, a rate-determining step still exists in spite of the presence of other exergic steps. When kinetic rate constants for more than one elementary step appear in the rate expression, we refer to all such elementary steps as "kinetically relevant" or "kinetically significant" steps, because any changes in their rate constants would influence the overall rate of the catalytic cycle. By this more general definition, which also includes as a special case those sequences controlled by only one exergic step, we conclude that solvents must influence rate constants and activated complexes involved

in kinetically relevant steps in order to influence the overall rate of a catalytic reaction sequence.

Boudart and Tamaru [13] also noted that many catalytic cycles involve an entry and an exit elementary step, both of which are one way (irreversible) exergic steps, and the exit step involves a most abundant reactive intermediate (MARI).

$$* + A \overset{k_{\text{entry}}}{\rightarrow} \cdots\cdots\cdots B \overset{k_{\text{exit}}}{\rightarrow} * + B*$$
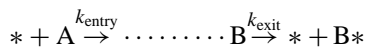
where $*$ denotes an active site. Such a reaction cycle communicates with its surroundings only through entry and exit steps. Solvent effects will depend then on whether kinetically relevant activated complexes are those involved in an entry step with a rate constant k_{entry} or in a desorption-reaction exit step with a rate constant k_{exit}. In these cases, activated complexes may be influenced via the same solvation effects as reactant or product molecules in the fluid phase, especially when transition states resemble solvated reactants. This usually occurs in early transition states for exothermic adsorption steps or late transition states for endothermic desorption steps. The olefin hydrogenation sequence first proposed by Horiuti and Polanyi [14] provides an excellent example of one such two-step mechanism.

3. Cyclohexene Hydrogenation on Supported Metal Catalysts

Here, we refer to the work of Madon et al. [15] and of Gonzo and Boudart [16] for the hydrogenation of cyclohexene (R) in a liquid phase using supported Pt and Pd catalysts, respectively. On supported Pt catalysts, Madon et al. [15] found that cyclohexene hydrogenation turnover rates measured at a given H_2 pressure depended on the chemical identity of the solvent used. Only when they expressed reaction rates in terms of the concentration of dissolved H_2 in each solvent, did reaction rate constants become independent of the nature of the liquid phase. Here reaction rates increased with increasing liquid phase H_2 concentration which depends on the nature of the liquid, unlike the thermodynamic activity of dissolved H_2 which does not. This example represents one of the few clearly documented cases of such solvent effects for reactions catalyzed by solids and one in which diffusion

restrictions were rigorously and explicitly ruled out. At first glance, these results appear to contradict the arguments based on transition state theory presented earlier in this manuscript.

On supported Pd catalysts [16], Gonzo and Boudart found that cyclohexene turnover rates did not depend on the identity of the liquid phase. Here, H_2 thermodynamic activities, instead of concentrations, led to rate constants that did not depend on the solvent used. Since thermodynamic activities for a given H_2 pressure do not depend on the nature of a solvent, but are only a function of gas phase H_2 partial pressure, H_2 solubility or the nature of the solvent did not play a role in influencing reaction rates. It is remarkable that the same hydrogenation reaction on two similar noble metal catalysts shows such different solvent effects. These different effects may be reconciled within the context of transition state theory by recognizing that the kinetically relevant steps in the Horiuti–Polanyi catalytic cycle [14] are different on Pt and Pd catalysts.

Cyclohexene hydrogenation on Pt proceeds via the elementary steps in Sequence 1, in which g, l, and p denote components in the gas phase, dissolved in the liquid, and physisorbed on the catalyst surface, respectively. Madon et al. [15] provided evidence for the sequence in Sequence 1, and details are given in the original reference. The reaction rate is zero order in cyclohexene and first order in H_2; the kinetically relevant rate constant is k_3, and it is the rate constant for an entry step (k_{entry}). Step 3 is therefore the exergic rate-determining step by the definition of Boudart and Tamaru. A transition state analysis of this rate constant is given in (14); here, we review some of the details because the approach used is relevant to other examples in this manuscript.

Sequence 1: Cyclohexene (R) Hydrogenation on Pt
1. $H_2^g \rightleftharpoons H_2^l$
2. $H_2^l \rightleftharpoons H_2^p$
3. $H_2^p + ** \xrightarrow{k_3} 2H*$
4. $R + ** \rightleftharpoons *R*$
5. $*R* + H* \rightleftharpoons RH* + **$
6. $RH* + H* \xrightarrow{k_6} RH_2 + **$

For the exergic Step 3 in Sequence 1, we introduce the activated complex ‡ as follows:

$$H_2^p + ** \rightleftharpoons \ddagger \rightarrow 2H* \tag{6}$$

From Eq. (2), we obtain

$$r = \frac{k_B T}{h} \frac{K^\ddagger}{\gamma_\ddagger} a_{H_2^p} a_{**} \tag{7}$$

where $K^\ddagger$, as defined earlier, is the equilibrium constant for the reactants in the ground state converting to the activated complex in Eq. (6). This constant is defined in terms of the change in the standard Gibbs free energy $\Delta G^{0\ddagger}$ for $H_2^p + ** \rightleftharpoons \ddagger$. Therefore,

$$K^\ddagger = \exp\left(-\frac{\Delta G^{0\ddagger}}{R_g T}\right) \tag{8}$$

This standard free energy change is related to the chemical potentials of H_2^p, $**$ and $\ddagger$ in their standard state (chosen arbitrarily).

$$\Delta G^{0\ddagger} = \mu_\ddagger^0 - \mu_{H_2^p}^0 - \mu_{**}^0 \tag{9}$$

This term depends on temperature and on the definition of standard states for each component. Standard states for pure components are a matter of convenience as long as consistency is maintained throughout the treatment. We use a standard state of unit fugacity (1 bar) for each component as a pure species.

Assuming that the solvent does not react with or chemisorb on surface sites, f_{**} is independent of the solvent, and for convenience we write

$$a_{**} = \frac{f_{**}}{f_{**}^0} = 1 \tag{10}$$

Expressing all activities in terms of concentrations and activity coefficients, we rewrite Eq. (7) to give

$$r = \frac{k_B T}{h} \exp\left(\frac{-\Delta G^{0\ddagger}}{R_g T}\right) \times \frac{\gamma_{H_2^p} C_{H_2^p}}{\gamma_\ddagger} \tag{11}$$

Since H_2 in the precursor state is in equilibrium with H_2 dissolved in the liquid phase, we have

$$K_H = \frac{a_{H_2^p}}{a_{H_2^l}} \tag{12}$$

Substituting into Eq. (11), we obtain

$$r = \frac{k_B T}{h} \exp\left(\frac{-\Delta G^{0\ddagger}}{R_g T}\right) K_H \times \frac{\gamma_{H_2^l} C_{H_2^l}}{\gamma_\ddagger} \tag{13}$$
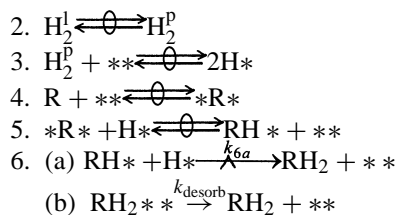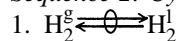
The kinetically relevant step (Step 3) is an exothermic adsorption reaction with a low activation energy [15]; as a result, the activated complex for Step 3 occurs early along the reaction coordinate and resembles the solvated H_2 reactant. Madon et al. [15] argued that the influence of the catalyst on this early transition state is small and that the activated complex closely resembles a solvated H_2 molecule, with an almost intact H–H bond and very weak H–surface bonds. In this case, the solvent would influence the activated complex and the H_2 molecules dissolved in the liquid to the same extent. Consequently, activity coefficients $\gamma_{H_2^l}$ and $\gamma_{\ddagger}$ in Eq. (13) cancel to give

$$r = \frac{k_B T}{h} \exp\left(\frac{-\Delta G^{0\ddagger}}{R_g T}\right) K_H C_{H_2^l} \qquad (14)$$

The rigorous application of transition state theory for a reaction in a non-ideal mixture showed reaction rates to be proportional to the concentration of H_2 in the liquid. But this occurred only because an entry adsorption step was the only kinetically relevant elementary step in a reaction sequence and led to a fortuitous cancellation of activity coefficients. The reaction rate depends on the solvating power of the liquid for cyclohexene hydrogenation on Pt [15] because the liquid solvates the activated complex involved in the rate-determining entry step. In general, for cases in which the exergic step is an entry exothermic step, the environment, gas or liquid, that contains reactants, may affect the resulting early transition state. In the extreme case of an activated complex that is nearly identical to the reactant, cancellation of activity coefficients leads to the apparent dependence of rates on concentration rather than on the thermodynamic activity of the reactant.

The catalytic cycle for cyclohexene hydrogenation on Pd [16] resembles that on Pt, but the hydrogen chemisorption entry step (Step 3) is quasi-equilibrated. Gonzo and Boudart [16] have discussed these elementary steps in detail. The reaction rate on Pd is zero order in cyclohexene and half order in H_2. In Sequence 2, we divide the exit step, involving the reactive desorption of RH∗, into two steps (6a and 6b) in order to preserve its elementary nature. The one-way exergic Step 6a is the rate-determining step [16].

Sequence 2: Cyclohexene (R) Hydrogenation over Pd
1. $H_2^g \overset{}{\underset{}{\rightleftharpoons}} H_2^l$

2. $H_2^l \overset{}{\underset{}{\rightleftharpoons}} H_2^p$
3. $H_2^p + \ast\ast \overset{}{\underset{}{\rightleftharpoons}} 2H\ast$
4. $R + \ast\ast \overset{}{\underset{}{\rightleftharpoons}} \ast R\ast$
5. $\ast R\ast + H\ast \overset{}{\underset{}{\rightleftharpoons}} RH\ast + \ast\ast$
6. (a) $RH\ast + H\ast \overset{k_{6a}}{\rightarrow} RH_2 + \ast\ast$

   (b) $RH_2 \ast\ast \overset{k_{desorb}}{\rightarrow} RH_2 + \ast\ast$

The relevant kinetic parameter for cyclohexene hydrogenation on Pd corresponds to the rate constant for the exergic exit step (k_{6a}). This step occurs via an activated complex

$$RH\ast + H\ast \overset{}{\underset{}{\rightleftharpoons}} \ddagger \rightarrow RH_2 \ast\ast$$
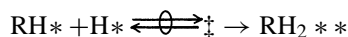
Using the same approach as for Pt catalysts and expressing all activities in terms of concentrations and activity coefficients, the rate of reaction on Pd is given by

$$r = \frac{k_B T}{h} \exp\left(-\frac{\Delta G^{0\ddagger}}{R_g T}\right) \times \frac{\gamma_{RH\ast} C_{RH\ast} \gamma_{H\ast} C_{H\ast}}{\gamma_{\ddagger}} \qquad (15)$$

where the change in the standard Gibbs free energy for $RH\ast + H\ast \overset{}{\underset{}{\rightleftharpoons}} \ddagger$ may be expressed in terms of chemical potentials for the corresponding standard states.

$$\Delta G^{0\ddagger} = \mu_{\ddagger}^0 - \mu_{RH\ast}^0 - \mu_{H\ast}^0 \qquad (16)$$

As noted earlier [15,16], RH∗ is the most abundant surface intermediate. Therefore, $C_{RH\ast} \sim L$, where L is the total surface concentration of active sites. For the case of a quasi-equilibrated sequence of hydrogen solvation and adsorption steps

$$H_2^g \overset{}{\underset{}{\rightleftharpoons}} H_2^l \overset{}{\underset{}{\rightleftharpoons}} H_2^p \overset{}{\underset{}{\rightleftharpoons}} 2H\ast \qquad (17)$$
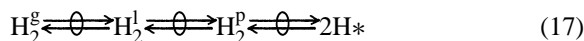
we obtain

$$K_H' = \frac{a_{H\ast}^2}{a_{H_2^g} a_{\ast\ast}} \qquad (18)$$

where K_H' is the product of the equilibrium constants for each of the elementary steps in Eq. (17). Substituting in Eq. (15), we have

$$r = L \exp\left(-\frac{\Delta G^{0\ddagger}}{R_g T}\right) \times \frac{\gamma_{RH\ast}}{\gamma_{\ddagger}} \sqrt{K_H' a_{\ast\ast} a_{H_2^g}} \qquad (19)$$

The most abundant reactive intermediate RH∗ and the activated complex formed when reacting with H∗ in Step 6a (Sequence 2) are predominantly influenced by their strong chemical bonds to Pd surface sites, and not

by solvation by the liquid phase. Therefore, the ratio $\gamma_{RH*}/\gamma_{\ddagger}$ (and a_{**}) cannot be influenced by the identity or the chemical properties of the solvent. And since the activity coefficient for H_2 in the gas phase is unity, Eq. (19) shows the experimentally observed half order rate dependence on gas phase hydrogen concentration.

$$r = L \exp\left(-\frac{\Delta G^{0\ddagger}}{R_g T}\right) \times \frac{\gamma_{RH*}}{\gamma_{\ddagger}} \sqrt{K'_H a_{**}} \sqrt{C_{H_2}^g} \quad (20)$$

Eq. (20) predicts that the rate coefficient and the turnover rate on Pd do not depend on the identity of the solvent, as observed experimentally [16]. Such a prediction would not be obtained from any rate expression written in terms of the concentration of dissolved hydrogen.

In this section, we have shown that for a reaction that proceeds on two metal surfaces via the same catalytic cycles, but with different kinetically relevant steps, the influence of the liquid phase and the *apparent* driving force for the reaction rates differ markedly. Only when reactants and activated complexes for kinetically relevant steps are solvated to an identical extent by the liquid, the activity coefficients for the reactant and for the activated complex fortuitously cancel. This gives the *appearance* of a kinetic process driven by concentration rather than the thermodynamic activity of dissolved reactants. Requirements for such cancellation of activity coefficients, as noted above, are quite stringent, thus making such cases unusual exceptions to the rigorous dependence of chemical reaction rates on the thermodynamic activities of reactants.

4. The formation and readsorption of olefins in the Fischer–Tropsch synthesis

Fischer–Tropsch (FT) synthesis [17,18] reactions form hydrocarbon chains from H_2 and CO on Ru, Co, and Fe surfaces. The active atoms reside on the surface of metal or carbide crystallites immersed within liquid hydrocarbons. At steady state, catalyst pores are filled with unreactive large paraffins formed by the reaction, while interparticle spaces may be swept with liquid or gaseous hydrocarbons depending on experimental conditions, the extent of reaction, and the reactor type (e.g. trickle bed, bubble column, or slurry reactors). Products form via two parallel reaction-desorption exit steps: (i) irreversible hydrogenation of adsorbed growing alkyl chains to form paraffins and (ii) reversible dehydrogenation (β-hydrogen abstraction) of alkyl chains followed by desorption of adsorbed olefins. The microscopic reverse of the latter exit step is the initiation of alkyl chains via the reintroduction of olefins into the chain growth pathway. Herrington [19] and Pichler et al. [20,21] first suggested that readsorption of olefins influence chain growth processes by reversing one of the chain termination steps. More recently, we have demonstrated the critical role of olefin readsorption and of diffusion restrictions within liquid-filled pores on FTS selectivity [22–27].

In this section, we consider the role of a liquid phase on the rate of α-olefin readsorption and chain initiation. Readsorption increases the product molecular weight and leads to non-Flory carbon number distributions [22–27]. We have rigorously described the observed decrease in chain termination probability with increasing chain size using a reaction-transport model that includes *the higher readsorption reactivity and the lower diffusivity of large olefins*. The combined effects of these two trends lead to the enhanced readsorption of the larger olefins, to the curvature in the Flory selectivity plots, and to disappearance of olefins from the heavier FTS products, as summarized in a recent review [27]. These diffusional restrictions lead to intraparticle gradients in olefin fugacity, to longer residence times within catalyst pellets, and consequently to higher olefin readsorption efficiency. Such physical effects prevent olefin equilibration between the gas and liquid phases in the reactor. They also give rise to site density effects on chain growth probability and product olefinicity, which cannot be explained by any chemical effects of the liquid on the solubility or readsorption probability of olefins. In spite of this, a research group at Shell [28,29] as well as others [30,31] have attributed observed non-Flory distributions to higher readsorption rates of larger olefins as a result of their higher solubility or higher physisorption tendency, which would lead to a higher concentration of the larger olefins near catalytic sites. These explanations are not only inconsistent with the observed site density effects, but also contradict, as we show below, predictions of readsorption rates from accepted kinetic treatments based on transition state theory.

Rigorous treatments of kinetics in multiphase reactors correctly express reaction rates in a liquid phase as a function of the virtual pressures of reactants and products [26]. Virtual pressure is defined as the gas phase pressure that would be in equilibrium with the prevalent local concentration of a given component in the liquid phase. This virtual pressure represents the fugacity of the component in the liquid phase, in view of the fact that the contacting gas phase is usually ideal. In such an accepted approach to the modeling of multiphase reactors, the solvating nature of inert paraffin liquids cannot influence the tendency of olefins to readsorb during FT synthesis, in contradiction with the recent claims [28–31]. Diffusional restrictions, which prevent the attainment of vapor–liquid equilibrium for these olefins, can give rise to liquid phase effects on FT synthesis rate or selectivity by introducing chemical potential gradients between the gas and liquid phases. The only other mechanism by which a liquid can influence the rate of a surface-catalyzed chemical reaction is by modifying the activated complexes involved in rate-determining elementary steps.

In the absence of concentration (or, more rigorously, fugacity) gradients introduced by intraparticle diffusion restrictions, phase equilibrium exists between a gas phase and the non-ideal liquid phase within which catalytic sites reside. In a previous study [32], we provided a straightforward example of the irrelevance of concentration as a kinetic driving force in FT synthesis. We measured rates and selectivities, during early times on stream, as the initially liquid-free pore space within small pellets (0.11–0.18 mm) gradually filled with the liquid products of FT synthesis. As the environment surrounding the sites evolved with time from a gas phase to a liquid phase, FT reaction rates and selectivities did not change, in spite of large concomitant changes in the H_2 and CO concentrations within catalyst pores. In larger pellets (0.85–1.7 mm), however, as pores became filled with liquids, CO diffusional restrictions became important and FT synthesis rate and C_{5+} selectivity decreased markedly with time. *A liquid phase gives rise to differences in fugacity and in kinetic driving force only when diffusion limitations prevent quasi-equilibrium between the gas and liquid phases, and not when the liquid, by the nature of its solvating interactions with reactants and products, changes reactant or product concentrations.* Diffusion processes are also driven by gradients in the fugacity or chem-
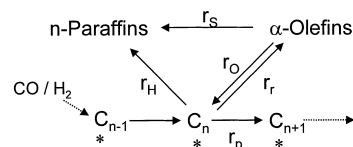

Fig. 1. Simplified scheme for hydrocarbon chain formation during FT synthesis.

ical potential of individual species [33]; the evolution of such gradients as a result of a liquid phase can substantially influence FT synthesis rates and selectivity.

In Fig. 1, we describe FT synthesis using a simplified and widely accepted chain growth scheme, which we have discussed in detail elsewhere [22].

Chain termination to paraffins (r_H) is irreversible, but olefins may readsorb ($r_{n,r}$) and re-initiate growing chains via the microscopic reverse of the β-hydrogen abstraction termination step that forms these olefins. The readsorption rate $r_{n,r}$ depends on chain length if the surrounding liquid influences olefins of varying sizes to different extents. The chain termination probability for a chain with n carbon atoms (β_n) is then given by

$$\beta_n = \frac{r_H + (r_O - r_{n,r})}{r_p} = \beta_H + \beta_{n,O}^{net} \tag{21}$$

where r_0 is the rate of termination as an olefin, r_p is the rate of propagation of the chain, and $(r_0 - r_{n,r})$ represents the net desorption rate for olefin molecules with n carbons. The paraffin chain termination probability β_H does not depend on chain size (Fig. 2a and b) [24,27]. This suggests that effects of chain size on overall (net) termination probabilities are not related to the rate of the (forward) chain termination steps. The overall chain termination probability, however, decreases with increasing chain size, because of a monotonic decrease in the net termination to olefins $\beta_{n,O}^{net}$ as chain size increases (Fig. 2a and b). This leads to the observed non-Flory distributions. Readsorption rates also influence the ratio, ψ_n, of α-olefins to paraffins in the products

$$\psi_n = \frac{r_O - r_{n,r}}{r_H} = \frac{\beta_{n,O}^{net}}{\beta_H} \tag{22}$$

which also decreases with increasing chain size (Fig. 3). These carbon number effects, as well as observed effects of reactor contact time, can be de-
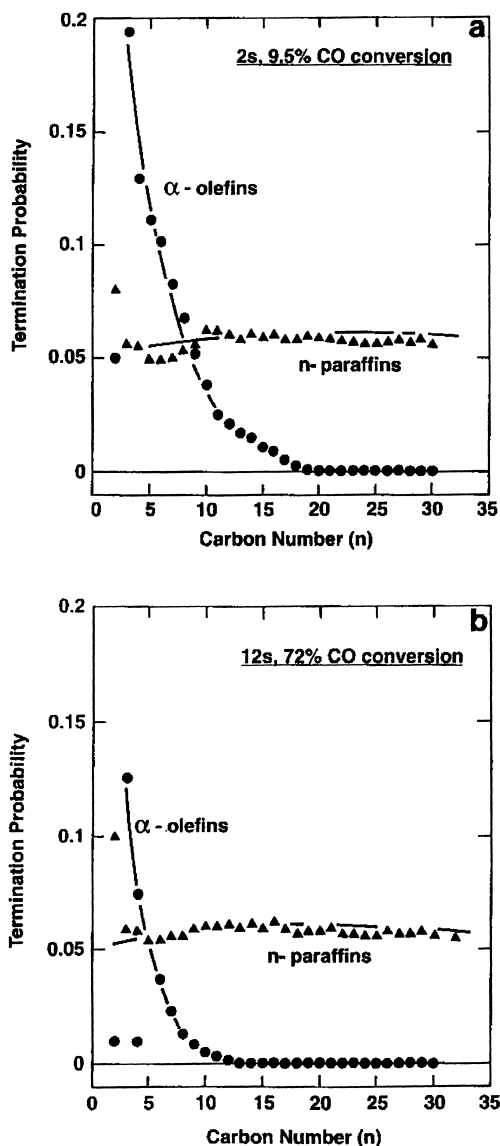
Fig. 2. Carbon number effects on olefin and paraffin chain termination probability. Catalyst: Co/TiO$_2$, 11.7 wt.% Co, and 1.5% Co dispersion, 473 K, 2000 kPa, H$_2$/CO = 2.1. (a) 2 s bed residence time, (b) 12 s bed residence time [26].

Fig. 3. Bed residence time and carbon number effects on the α-olefin to paraffin ratio. Same catalyst and conditions as in Fig. 2 [26].

scribed quantitatively by the higher readsorption rate constant of larger olefins and by their slower diffusion rates within liquid-filled catalyst pellets [22–27]. Below, we show that proposals based on changes in the solubility or physisorption energy with olefin size [28–31] are not consistent with thermodynamics or with trans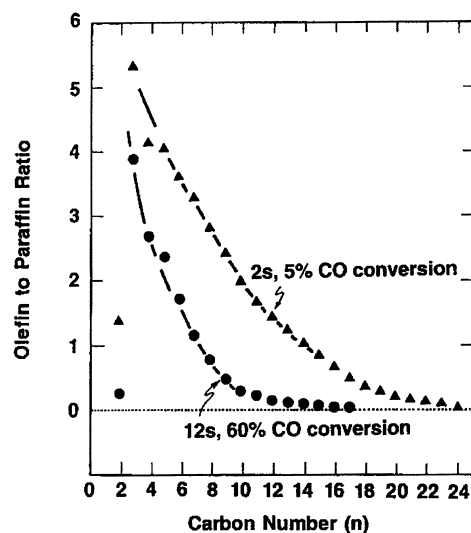ition state theory treatments of chemical reaction rates. The details follow the general approach used in the previous sections for cyclohexene hydrogenation reactions.

The only aspect of the FT synthesis mechanism relevant to our discussion is the exit step, consisting of the reversible reaction-desorption of surface alkyl species AH* as an olefin A. Sequence 3 is only a partial sequence of the elementary steps required for a FT synthesis turnover, but it contains all of the elements required to answer the question posed. Of course, the net rate of desorption of olefins and paraffins must always be balanced at steady state by the rate at which AH* is formed via entry steps involving the hydrogenation of CO on the catalytic surface.

Sequence 3
1. $AH* + * \rightleftharpoons A* + H*$
2. $A* \rightleftharpoons A_p + *$
3. $A_p \rightleftharpoons A_l$
4. $A_l \rightleftharpoons A_g$

A growing alkyl chain with *n* carbon atoms (AH*) is a half-hydrogenated olefin that forms an adsorbed olefin by eliminating H. This is the microscopic reverse of the first hydrogen addition to an adsorbed olefin in the Horiuti–Polanyi mechanism (see Sequence 1, step 5). Adsorbed olefins then desorb in step 2 into a physisorbed layer or precursor state A$_p$, which we

include as a possibility, even in the absence of any direct evidence for its existence or role, because it has been proposed by the Shell group [28,29]. The next two steps involve the desorption of the physisorbed olefin into the liquid phase to form A_l and then into the gas phase (A_g), which flows as bubbles or as a continuous gas phase in the space between catalyst pellets. The surface-catalyzed steps in Sequence 3 represent the microscopic reverse steps of the elementary steps in the Horiuti–Polanyi mechanism for olefin hydrogenation (Sequence 1) [14].

In the absence of transport restrictions, Step 4 in Sequence 3 is quasi-equilibrated during FT synthesis. Quasi-equilibrium of Step 3 is also expected in view of small physisorption enthalpies and two-way activation energies for adsorption–desorption steps in physisorption processes. A similar quasi-equilibrium argument is often made for chemisorption steps, even with their higher adsorption enthalpies, but we refrain from making this more restrictive assumption here and consider it below as a special case. The equality of chemical potential required for thermodynamic equilibrium for species i among several phases leads to

$$\mu_{A,g} = \mu_{A,l} = \mu_{A,p} \tag{23}$$

for olefins in the gas, liquid, and physisorbed phases during chain termination (desorption) to form olefins.

All reactions of olefins in the liquid or physisorbed phases occur via thermodynamic equilibration with chemisorbed olefins or with the activated complex involved in Step 1 (if this step is exergic). Therefore, the kinetic problem under consideration becomes a purely thermodynamic one, and it may be treated rigorously without considering explicitly the properties or concentrations of solvated or physisorbed olefins.

For completeness and without loss of generality, we consider two cases for the FT synthesis termination sequence shown in Sequence 3.

Case A: Step 2 is quasi-equilibrated and the net rate of desorption of olefins is given by the rate of the exergic Step 1.

Case B: The net rate is given by Step 2, which is the exergic step, while Step 1 is in quasi-equilibrium.

For Case A, using Eq. (23), we first apply the condition of equilibrium among liquid, gas, physisorbed, and chemisorbed phases to obtain

$$\mu_{A*} = \mu_{A,p} = \mu_{A,l} = \mu_{A,g} \tag{24}$$

This relates the gas and chemisorbed phases without explicitly considering intervening liquid and physisorbed phases. As a result, the thermodynamic activity of chemisorbed A (or its concentration for an ideal Langmuirian surface) is independent of the identity or even the presence of the liquid. We rewrite Sequence 3 by combining the last three steps.

Sequence 3, Case A
1. $AH* + * \underset{}{\overset{A}{\rightleftharpoons}} A* + H*$
2. $A* \underset{}{\overset{\theta}{\rightleftharpoons}} A_g + *$

The rate of the overall termination process can then be obtained by considering the net rate of the reversible exergic Step 1 in Case A using transition state theory. Using Eq. (2) for the forward (f) and reverse (r) steps leads to

$$r_{net} = r_{forward} - r_{reverse}$$

$$= \frac{k_B T}{h} \frac{1}{\gamma_\ddagger} \left[\exp\left(-\frac{\Delta G_f^{0\ddagger}}{R_g T}\right) a_{AH*} a_* \right.$$

$$\left. - \exp\left(-\frac{\Delta G_r^{0\ddagger}}{R_g T}\right) a_{A*} a_{H*} \right] \tag{25}$$

where $\Delta G_f^{0\ddagger}$ and $\Delta G_r^{0\ddagger}$ are changes in standard free energies of reaction for the forward and reverse steps of Step 1 in Sequence 3, and the overall free energy change is given by

$$\Delta G_1^0 = \Delta G_f^{0\ddagger} - \Delta G_r^{0\ddagger} \tag{26}$$

From the quasi-equilibrated Step 2 for Case A, we obtain

$$K_{eq,2} = \frac{a_{A_g} a_*}{a_{A*}} = \exp\left[\frac{-\Delta G_2^0}{R_g T}\right] \tag{27}$$

Finally, from Eqs. (25)–(27), we obtain

$$r_{net} = \frac{k_B T}{h} \frac{a_*}{\gamma_\ddagger} \exp\left(-\frac{\Delta G_f^{0\ddagger}}{R_g T}\right)$$

$$\times \left[a_{AH*} - \exp\left(\frac{\Delta G_1^0 + \Delta G_2^0}{R_g T}\right) a_{A_g} a_{H*} \right]$$

$$= \frac{k_B T}{h} \frac{a_*}{\gamma_\ddagger} \exp\left(-\frac{\Delta G_f^{0\ddagger}}{R_g T}\right) \left[a_{AH*} - \frac{C_{A_g} a_{H*}}{K_{overall}} \right] \tag{28}$$

where $K_{overall}$ represents the standard Gibbs free energy change for the overall reaction $AH* \rightleftharpoons A_g + H*$, and Eq. (28) does not explicitly contain any physisorbed or dissolved A.

In this treatment, activity coefficients for all surface intermediates become unity for ideal Langmuirian surfaces, but even for non-ideal surfaces, their values reflect only the non-ideality of the surface caused by intermolecular interactions among adsorbed species *without any additional effects imposed by the presence of a liquid phase or a physisorbed phase*. Therefore, unless a liquid is able to influence the properties of a catalytic surface by modifying the binding energy of adsorbed species, it cannot influence the rate of chain termination to olefins. In Case A, olefin solubility or physisorption tendency cannot influence in any way the rate of desorption or adsorption of olefins. Case A is much more likely to describe Sequence 3 than Case B (treated below), because of (a) the rapid nature of most non-dissociative adsorption–desorption processes, and (b) the accepted rate-determining nature of hydrogen addition and abstraction steps in related olefin hydrogenation and dehydrogenation reactions, respectively.

Case B presents a more provocative situation, because the exergic step involves the participation of reactant species within the liquid phase A_l or the physisorbed phase A_p. This treatment is unaffected by the presence or absence of a physisorbed phase, as can be confirmed easily by the reader. Because species solvated by the liquid are involved in the exergic exit step, it becomes possible for an activated complex to detect the presence of a liquid or a physisorbed layer, as in the case of cyclohexene hydrogenation on Pt. Since Step 2 in Sequence 3 is the exergic step for Case B.

Sequence 3, Case B,
1. $AH* + * \rightleftharpoons A* + H*$
2. $A* \rightleftharpoons A_p + *$
3. $A_p \rightleftharpoons A_g$

the net desorption rate to form olefins is given by the rate of the reversible Step 2. Using Eq. (2) for the forward (f) and reverse (r) steps of Step 2, the net rate becomes

$$r_{net} = \frac{k_B T}{h\gamma_\ddagger} \exp\left(-\frac{\Delta G_f^{0\ddagger}}{R_g T}\right)\left[a_{A*} - \frac{C_{A_g} a_*}{K_{overall}}\right] \quad (29)$$

where $K_{overall}$ represents the standard Gibbs free energy change for the combined Steps 2 and 3 in Case B ($A* \rightleftharpoons A_g + *$). This expression does not explicitly include any concentrations of dissolved or physisorbed species or any of their thermodynamic properties.

An effect of the liquid on the activity coefficient for the activated complex cannot be ruled out here, because the activated complex occurs along a reaction coordinate that originates within the liquid phase (or the physisorbed phase). As a result, the activated complex can be stabilized by such a phase. Thus, a kinetic effect of the solvent is possible, but only if the activated complex is influenced by the solvent, and not because of any changes in the thermodynamic activities of olefins in liquids with different solvating properties, or in the physisorbed phase, or when no liquid is present. The argument remains unchanged if we consider instead olefins with different chain size, which have different solubility in a given solvent.

Solvation of the activated complex by the liquid in Case B is stronger for complexes formed early in the reaction coordinate, a situation common for non-activated chemisorption processes. In the limit of activated complexes that closely resemble reactants, solvation effects become identical for the reactant arriving from the external phase and for the activated complex. Then, activity coefficients become similar for the two species and they cancel each other in the rate expression. We thus obtain, as we did earlier for cyclohexene hydrogenation on Pt, a readsorption rate that becomes proportional to the concentration of olefins in the liquid or physisorbed phase. From Eq. (29) we obtain

$$r_{net} = \frac{k_B T}{h} \exp\left(-\frac{\Delta G_f^{0\ddagger}}{R_g T}\right)\left[\frac{a_{A*}}{\gamma_\ddagger} - \frac{C_{A_l} a_*}{K_{overall}}\right] \quad (30)$$

However, the activity coefficient for the activated complex in the forward reaction term of Eq. (30) does not disappear, because the reactants involved in the desorption step are influenced by their strong interactions with the catalytic surface rather than by their much weaker interactions with the liquid solvent. At first glance, this expression appears to support the proposal that a higher liquid phase concentration of an olefin, as a result of its higher solubility in the liquid, would decrease its net rate of desorption by increasing the

readsorption rate, albeit only for the unlikely instance of Case B.

In fact, Eqs. (29) and (30) predict the opposite trend for Case B. As we explain below, a higher solubility for reactants and the consequent stronger solvation of activated complexes actually lead to higher net olefin desorption rates and therefore to an increase in the chain termination probability with increasing chain size. In contrast, experimental chain termination probabilities on Co, Ru, or Fe always decrease or remain constant as the carbon number increases. The predicted effects of increasing solvation, if such effects were important (as in Case B), would be opposite to those stated by the Shell group [28,29], whether such solvation effects arise from interactions within a liquid or a physisorbed phase.

The chemical potential for an olefin at vapor–liquid equilibrium is identical in the liquid and gas phases,

$$\mu_g^0 + R_g T \ln \frac{f_g}{f_g^0} = \mu_l^0 + R_g T \ln \frac{f_l}{f_l^0} \qquad (31)$$

and since the gas phase is assumed to be ideal, we obtain

$$P_g = \exp\left(-\frac{\Delta\mu^0}{R_g T}\right) \gamma_l C_l \qquad (32)$$

Clearly, for a given pressure P_g, stronger solvation leads to a higher solute concentration C_l in the liquid; thus, the better the solvent or the more soluble the olefin, the lower the activity coefficient γ_l for the solute. We now return to Eq. (29) and similarly consider (for the exergic Step 2) the effect of stronger solvation on the net rate of chain termination to olefins during FT synthesis. As the value of $\gamma_{\ddagger}$ decreases because of these stronger solvation effects, both forward and reverse olefin desorption rates increase by an identical factor, and the net desorption rate and the chain termination probability increases. Intuitively this is obvious, since stabilization of an activated complex by a better solvent increases the rate of both forward and reverse elementary reactions to the same exact extent. *Therefore, a better solvent increases the rate of a given step in the direction allowed by thermodynamics; this is of course the direction observed for a given reaction at steady-state.* In FT synthesis, that direction is *always* towards the net desorption of olefins, because olefins are formed from H_2–CO

mixtures during the Fischer–Tropsch synthesis. These conclusions are unaffected by the possibility that there is a net consumption of olefins of a size n at a given point in the reactor, because the integrated net rate of chain termination along a reactor, as given by Eq. (29) is always positive in FT synthesis reactions.

The ability of a liquid to "solvate" one or more reactants is inconsequential in kinetic or thermodynamic treatments of chemical reactions unless it also solvates the activated complex in an exergic step. When it does (infrequently), because the exergic step is an entry or exit step in the surface-catalyzed sequence, a better solvent increases the rate of the catalytic reaction in the net direction observed at steady-state. In such unusual instances, a better solvent (or a more soluble olefin) would lead to a higher net desorption rate in FT synthesis, not to lower net desorption rates as claimed in [28–31]. Condensed FT synthesis products influence synthesis rates and selectivities by introducing transport restrictions. Such restrictions are unrelated to solubility effects, but instead reflect the diffusivity and reactivity of olefins present within this liquid phase and the physical and chemical attributes (porosity, pellet size, active site density) of the catalyst [22–27].

5. Reactions on zeolite catalysts

In the previous examples, we have shown how a non-ideal environment imposed by a liquid solvent influences, under some circumstances, rates of chemical reactions. Here, we explore solvating effects of microporous structures such as zeolites.

Rabo et al. [34] first proposed that unusually high concentrations of reactants existed within zeolites due to strong polarization interaction between zeolite crystals and adsorbing molecules. Fraissard [35], using ^{129}Xe NMR, also indicated a high apparent pressure of reactants within zeolites. Derouane et al. [36] used their confinement model to provide a rationale for such high intrazeolitic concentrations, suggesting that surface curvature of zeolite pores influences heats of adsorption and thus chemical reaction rates and selectivities. Derouane explored this confinement concept for various catalytic reactions [37] and more recently, with Chang [38], for the adsorption of bases. For paraffin cracking, Haag [39], Narbeshuber et al. [40], Kotrel et. al [41], and Babitz et al. [42] attributed differences

in reaction rates between different zeolites or different reactants to intrazeolitic reactant enrichment, which depends on the nature of the molecule and of the zeolite host, rather than to differences in the strength of zeolitic Brønsted acid sites. Because of such strong interactions within zeolites, Derouane [37], Haag [39] and Kotrel et al. [41] proposed that paraffin cracking rates in zeolites should be defined by

$$r = k \bar{K} C_P \tag{33}$$

where k is the rate constant for cracking and $\bar{K}$ is the adsorption equilibrium constant, denoted by Kotrel et al. [41] as the enrichment constant.

Since zeolites can "solvate" molecules trapped within their confined channel structure [37,43–45], observed differences in reactant concentrations between gas phase and zeolite channels are reminiscent of the solvating effects of liquid solvents discussed earlier. Reactant molecules within zeolite cavities and channels reside within a thermodynamically non-ideal phase, and the concentration of these reactants is a direct consequence of interphase equilibrium between the intrachannel and external phases. Therefore, the chemical potential of a reactant in the gas phase and within the zeolite structure must be equal.

$$\mu_{gas} = \mu_{zeolite} \tag{34}$$

As with liquid solvents, zeolite solvation effects may influence reactants, products, and activated complexes. But a zeolite may not only "solvate" activated complexes occurring early in the reaction cycle, but also the active site itself and influence all chemical transformations and elementary steps occurring on such sites. In effect, a site within a zeolite channel may resemble those in homogeneous organometallic complexes in that "ligands" (the zeolite framework) that stabilize the active site also solvate the reactant and product molecules as they arrive or depart. From Eq. (31), we obtain

$$P_{gas} = \exp\left(-\frac{\Delta\mu^0}{R_g T}\right) \gamma_z C_z \tag{35}$$

As before, for a given pressure P_{gas} in the gas phase, higher solubility within a zeolite leads to a higher solute concentration C_z and therefore to a lower value of the activity coefficient for the solute. If concentrations within zeolites are large, then activity coefficients must compensate and be small. *Only if γ_z*

cancels in a rate expression will a high intrazeolitic concentration lead to proportionally higher catalytic rates. Again, we examine these effects using transition state theory to determine under what conditions reaction rates depend on reactant concentration or thermodynamic activity within zeolite channels. Since if the latter holds, high concentrations within zeolites would not lead to proportionally high reactivity. The analysis shown below is general and may be readily extended to zeolite-catalyzed reactions other than paraffin cracking.

We analyze the case of a paraffin entering a zeolite channel, interacting with a Brønsted acid site, and cracking to form smaller molecules. We seek plausible reaction pathways that explain the dependence of cracking rates on intrazeolite paraffin concentrations or on thermodynamic activities. A paraffin in the external gas phase is first absorbed into a thermodynamically non-ideal zeolite phase, just as it would dissolve in a liquid phase. This step is quasi-equilibrated, and the chemical potentials of a paraffin in the external fluid phase and in the zeolite channels are therefore identical. Once a paraffin is absorbed (or solvated) within the zeolite, it enters the reaction pathways described by the two mechanistic options proposed below.

In Sequence 4, Case 1, paraffins from the gas phase (P_g) absorb within a zeolite (P_z) and react on a Brønsted acid site (H^+Z) to give products. Step 2 is the exergic step.

Sequence 4, Case 1
1. $P_g \overset{0}{\underset{\longrightarrow}{\rightleftharpoons}} P_z$
2. $P_z + H^+Z \overset{0}{\underset{\longrightarrow}{\rightleftharpoons}} \ddagger \rightarrow$ Products

As before, using Eq. (2), we obtain a rate expression for paraffin cracking.

$$r = \frac{k_B T}{h} \exp\left(-\frac{\Delta G^{0\ddagger}}{R_g T}\right) \times \frac{\gamma_{H^+Z}}{\gamma_{\ddagger}} C_{H^+Z} \gamma_{P_z} C_{P_z} \tag{36}$$

where $\Delta G^{0\ddagger}$ is the standard free energy change for the reaction $P_z + H^+Z \overset{0}{\underset{\longrightarrow}{\rightleftharpoons}} \ddagger$. We choose a hypothetical and arbitrary standard state of unit fugacity (1 bar) for each component as a pure species.

The solvating effect of zeolite channels on the activated complex, which involves a surface proton and a solvated paraffin to form a protonated transi-

tion state, is likely to differ significantly from the solvation effects on an absorbed paraffin. Therefore, activity coefficients in Eq. (36) are unlikely to cancel. Since paraffins in the gas phase are in thermodynamic equilibrium with paraffins within zeolite channels, the resulting equality of chemical potentials in the two phases leads to

$$K_z = \frac{\gamma_{P_z} C_{P_z}}{C_{P_g}} \tag{37}$$

which, when substituted into Eq. (36), gives

$$r = \frac{k_B T}{h} \exp\left(-\frac{\Delta G^{0\ddagger}}{R_g T}\right) \frac{\gamma_{H^+Z}}{\gamma_{\ddagger}} K_z C_{H^+Z} C_{P_g} \tag{38}$$

Therefore, for Case 1 the rate is proportional to gas phase concentration of reactants or to their thermodynamic activity within the zeolite, and not to the intrazeolitic paraffin concentration. Note that the rate constant, for reasons stated earlier and unlike in the case of inert solvents, depends on the zeolite channel structure and on the acid strength of the sites that reside within this channel structure.

We examine a second possibility (Sequence 4, Case 2) for which we introduce a precursor phase (P_{zr}) within the zeolite, which proceeds to react with a Brønsted acid site. The formation and stability of a precursor species would depend on the zeolite used. In this step, a paraffin is oriented in the right conformation by the zeolite in the vicinity of a Z–OH group. Then, as the H in the Z–OH group attains a higher energy state with increased charge polarization, the precursor paraffin reacts with the H^+.

Sequence 4, Case 2
1. $P_g \overset{}{\underset{}{\rightleftharpoons}} P_z$
2. $P_z \overset{}{\underset{}{\rightleftharpoons}} P_{zr}$
3. $P_{zr} + H^+Z \overset{}{\underset{}{\rightleftharpoons}} \ddagger \rightarrow$ Products

Using the same approach as Case 1, the rate is given by

$$r = \frac{k_B T}{h} \exp\left(-\frac{\Delta G^{0\ddagger}}{R_g T}\right) \times \frac{\gamma_{H^+Z} C_{H^+Z} \gamma_{P_{zr}} C_{P_{zr}}}{\gamma_{\ddagger}} \tag{39}$$

and, as in Case 1, activity coefficients do not cancel. Since P_z and P_{zr} are in equilibrium, we have

$$K_r = \frac{a_{P_{zr}}}{a_{P_z}} = \frac{\gamma_{P_{zr}} C_{P_{zr}}}{\gamma_{P_z} C_{P_z}} \tag{40}$$

We propose that P_z and the precursor P_{zr} reside within the same local zeolite environment near an active site, and they are similarly solvated by the zeolite environment. As a result, their respective activity coefficients are similar and

$$\frac{\gamma_{P_{zr}}}{\gamma_{P_z}} = 1 \tag{41}$$

Eq. (39) then becomes

$$r = \frac{k_B T}{h} \exp\left(-\frac{\Delta G^{0\ddagger}}{R_g T}\right) \times K_r \frac{\gamma_{H^+Z}}{\gamma_{\ddagger}} C_{H^+Z} C_{P_Z} \tag{42}$$

In Case 2, the rate becomes proportional to the paraffin concentration within the zeolite channels, *but only if Eq. (41) accurately describes solvation by the zeolite.*

In both Eq. (38) and Eq. (42), several terms depend on the identity of the zeolite. Eq. (42), for example, may be re-written as

$$r = \frac{k_B T}{h} K_r \frac{\gamma_{H^+Z}}{\gamma_{\ddagger}} C_{H^+Z} \exp\left(\frac{\Delta S^{0\ddagger}}{R_g}\right)$$
$$\times \exp\left(-\frac{\Delta H^{0\ddagger}}{R_g T}\right) C_{P_Z} \tag{43}$$

This expression may be separated into the pre-exponential factor and activation energy terms.

$$r = A \exp\left(-\frac{\Delta H^{0\ddagger}}{R_g T}\right) C_{P_Z} \tag{44}$$

Pre-exponential factors A have traditionally not been emphasized in catalytic cracking, but they clearly depend (as shown by Eq. (43)) on the properties of the zeolite channels and of acid sites. Eq. (43) contains the $\gamma_{\ddagger}$ term in the pre-exponential factor, reflecting the importance of zeolite properties on transition states. The ratio $\gamma_{H^+Z}/\gamma_{\ddagger}$ and equilibrium constant K_r (or K_z) are important variables in zeolite catalysis.

In this last section, we have used transition state theory to rationalize the possible role of intrazeolitic concentration or thermodynamic activity of reactants on chemical reaction rates. More definitive experimental evidence is required in order to choose between Cases 1 and 2. Though clearly other mechanistic choices may also describe experimental results, the two sequences presented here appear to be reasonable and straightforward possibilities. All mechanisms of reactions on

zeolites should be scrutinized for consistency with experimental results using the framework provided by transition state theory as applied to thermodynamically non-ideal environments.

6. Conclusions

Rates of chemical reactions depend on thermodynamic activities or fugacities of reactants and products. Concentrations may only be used for ideal systems or under special conditions discussed in this paper. Chemical reactions on surfaces cannot detect the presence or the chemical identity of a contacting fluid phase unless the liquid

  a. participates in the solvation of kinetically relevant adsorbed intermediates or activated complexes;
  b. imposes concentration gradients through diffusion restrictions and, thus, changes the local chemical potential of reactants and products near catalytic surfaces.

When a solvent or some other condition introduces non-ideality into the reacting system, transition state theory may be used to rigorously describe effects of non-ideal behavior on reaction rates. Rates of catalytic reactions depend on the presence of a solvent only when it influences activated complexes involved in kinetically significant steps (defined as those steps whose rate constants appear in the overall rate expression) in a catalytic cycle. When a liquid solvates reactants and activated complexes to an identical extent, a fortuitous cancellation of activity coefficients leads to reaction rates that depend on the concentration of the reactant in a solvent. Such a case arises when exothermic adsorption steps are rate-determining and involve activated complexes that occur early along the reaction coordinate; as a result, complexes may be solvated to the same extent as the solvated adsorbing molecules. For liquid phase hydrogenation of cyclohexene on Pt, the rate-determining step is the dissociative adsorption of H_2, and this leads to identical solvation of the H_2 molecule and of the activated complex. Consequently, activity coefficients cancel and the rate on Pt depends on liquid phase H_2 concentration. On Pd, the rate-determining step involves surface reactions occurring after H_2 chemisorption, and the activated complex of the kinetically relevant step is influenced only by the

catalytic site. Here, activity coefficients do not cancel, and the hydrogenation rate on Pd depends on the thermodynamic activity of hydrogen in the liquid phase.

Fischer–Tropsch synthesis provides another example where a liquid phase influences reaction rates of the readsorption of product olefins which initiate hydrocarbon chains. Higher olefin readsorption rates of larger olefins are not the result of higher solubility in the liquid phase. Transition state theory shows that increasing olefin solubility is either unimportant for olefin readsorption, or, under certain circumstances, would actually increase the tendency of an adsorbed olefin to desorb rather than of solvated olefins to readsorb. The olefin solubility-physisorption model proposed by Kuipers et al. [28,29] and others [30,31] is inconsistent with transition state theory and with experimental observations. Instead, the liquid paraffin phase within catalyst pores introduces an intraparticle transport limitation on the olefin products as they exit these pores. These diffusion limitations induce fugacity gradients that lead to the observed enhanced olefin adsorption as olefin size increases within catalyst pores.

In our final example, a zeolite, rather than a liquid, causes non-ideal behavior. A paraffin in an external fluid phase is absorbed into zeolite channels while maintaining equilibrium between the external fluid and the absorbed phases. Therefore rates of reactions within zeolites should be proportional to the thermodynamic activities of reactants within the zeolite. Using paraffin cracking as an example, we have proposed a case, where due to cancellation of activity coefficients, concentration rather than activity of a reactant in the zeolite describes reaction rates. If such cancellation does not occur, thermodynamic activities of reactants must be used.

Non-ideal behavior with zeolites is different from heterogeneous catalysis in liquid solvents in that a zeolite may solvate an active site, for example a Brønsted acid site, and the transition state of any elementary step in a catalytic cycle. This behavior of zeolites is similar to that of homogeneous catalysts where, often, chelating organic moieties are bonded to metal atom catalysts which are solvated in strongly interacting solvents. Solvent effects and the fortuitous cancellation of activity coefficients are much more likely in homogeneous catalysis leading to the apparent relevance of concentrations in rate expressions. In heterogeneous

catalysis, ligands are provided by the bulk atomic structure of the solid site, and contacting liquids provide molecular interactions and solvating effects that are much weaker except in the case of zeolites.

References

[1] Th. De Donder, L'Affineté, Gauthier-Villars, Paris, 1927, p. 43.

[2] I. Prigogine, R. Defay, Chemical Thermodynamics, D. H. Everett, Trans., Longmans, London, 1954, p. 38.

[3] M. Boudart, G. Djéga-Mariadassou, Kinetics of Heterogeneous Catalytic Reactions, Princeton University Press, Princeton, New Jersey, 1984 (Chapter 3).

[4] M. Boudart, Kinetics of Chemical Processes, Prentice-Hall, New Jersey, 1968, pp. 33–55.

[5] K. Denbigh, The Principles of Chemical Equilibrium, Cambridge University Press, Cambridge, UK, 1981 (Chapters 9 and 10).

[6] V. Gutmann, The Donor–Acceptor Approach to Molecular Interactions, Plenum, New York, 1978.

[7] J. P. Collman, L. S. Hegedus, J. R. Norton, R. G. Finke, Principles and Applications of Organotransition Metal Chemistry, University Science Books, Mill Valley, CA, 1987.

[8] H. Eyring, E.M. Eyring, Modern Chemical Kinetics, Reinhold, New York, 1963, pp. 29–50.

[9] J.B. Butt, Reaction Kinetics and Reactor Design, 2nd Edition, Marcel Dekker, New York, 2000, pp. 113–150.

[10] C.A. Eckert, M. Boudart, Chem. Eng. Sci. 18 (1963) 144.

[11] E. Whalley, Disc. Faraday Soc. 22 (1956) 148.

[12] J. Horiuti, J. Res. Inst. Catal., Hokkaido Univ. 5 (1957) 1.

[13] M. Boudart, K. Tamaru, Catalysis Lett. 9 (1991) 15.

[14] J. Horiuti, M. Polanyi, Trans. Faraday Soc. 30 (1934) 1164.

[15] R.J. Madon, J.P. O'Connell, M. Boudart, AIChE J. 24 (1978) 904.

[16] E.E. Gonzo, M. Boudart, J. Catal. 52 (1978) 462.

[17] M. Dry, in: J. R. Anderson, M. Boudart (Eds.), Catalysis, Science and Technology, Vol. 1, Springer, New York, 1981 (Chapter 4).

[18] R.B. Anderson, The Fischer–Tropsch Synthesis, Academic Press, New York, 1984.

[19] E.F.G. Herrington, Chem. Ind., 1946, pp. 347.

[20] H. Pichler, H. Schulz, M. Elstner, Brennstoff-Chem. 48 (1967) 78.

[21] H. Pichler, H. Schulz, F. Hojabri, Brennstoff-Chem. 45 (1964) 215.

[22] E. Iglesia, S.C. Reyes, R.J. Madon, J. Catal. 129 (1991) 238.

[23] R.J. Madon, S.C. Reyes, E. Iglesia, J. Phys. Chem. 95 (1991) 7795.

[24] R.J. Madon, E. Iglesia, J. Catal. 139 (1993) 576.

[25] R.J. Madon, E. Iglesia, S.C. Reyes, in: S.L. Suib, M.E. Davis (Eds.), Selectivity in Catalysis, ACS Symposium Series, Vol. 517, 1993, p. 383.

[26] E. Iglesia, S.C. Reyes, R.J. Madon, S.L. Soled, Adv. Catal. Relat. Subj. 39 (1993) 221.

[27] E. Iglesia, Appl. Catal. 161 (1997) 1.

[28] E.W. Kuipers, I.H. Vinkenburg, H. Oosterbeek, J. Catal. 152 (1995) 137.

[29] E.W. Kuipers, C. Scheper, J.H. Wilson, I.H. Vinkenburg, H. Oosterbeek, J. Catal. 158 (1996) 288.

[30] G.P. van der Lann, A.A. Beenackers, Catal. Rev. Sci. Eng. 41 (1999) 255.

[31] G.P. van der Lann, A.A. Beenackers, Stud. Surf. Sci. Catal. 119 (1998) 179.

[32] R.J. Madon, E. Iglesia, J. Catal. 149 (1994) 428.

[33] J. Karger, D. M. Ruthven, Diffusion in Zeolites and Other Microporous Solids, Wiley, New York, 1992, pp. 70–86.

[34] J. Rabo, R.D. Bezman, M.L. Poutsma, Acta Phys. Chem. (Hung.) 24 (1978) 39.

[35] J. Fraissard, Stud. Surf. Sci. Catal. 5 (1980) 343.

[36] E.G. Derouane, J-M. Andre, A.A. Lucas, J. Catal. 110 (1988) 58.

[37] E.G. Derouane, J. Mol. Catal. A. 134 (1998) 29.

[38] E.G. Derouane, C.D. Chang, Micro. Meso. Mater. 35 (2000) 425.

[39] W.O. Haag, Stud. Surf. Sci. Catal. 84 (1994) 1375.

[40] T.F. Narbeshuber, H. Vinek, J.A. Lercher, J. Catal. 157 (1995) 388.

[41] S. Kotrel, M.P. Rosynek, J.H. Lunsford, J. Phys. Chem. B. 103 (1999) 818.

[42] S.M. Babitz, B.A. Williams, J.T. Miller, R.Q. Snurr, W.O. Haag, H.H. Kung, Appl. Catal. A 179 (1999) 71.

[43] J.H. de Boer, J.F.H. Custers, Z. Phy. Chem., Abt B, 25 (1934) 225.

[44] H. Stach, H. Thamm, J. Jaenchen, K. Fiedler, W. Schirmer, in: Proceedings of 6th International Zeolite Conference, Reno, USA, 1983, p. 225.

[45] H. Stach, U. Lohse, H. Thamm, W. Schirmer, Zeolites 6 (1986) 74.